MESHFREE MULTISCALE METHOD WITH PARTIALLY EXPLICIT TIME DISCRETIZATION

Nikiforov D. Ya.

Abstract In this paper, a multiscale approach with partially explicit time discretization is proposed. The idea is to use a partially explicit time scheme, considering a filtration problem in a fractured medium, where the implicit scheme is used for nodes whose subdomains contain fractures, and the explicit scheme is used for all others. In this way, it is possible to use a time step that is independent of the diffusion coefficient for fractures. Numerical results demonstrating high accuracy of calculations are presented.

Key words: multiscale methods, meshfree methods, partially explicit scheme, mathematical modeling, fractured domain, finite element method.

AMS Mathematics Subject Classification: 97M99, 76S05, 78M10, 65M50.

DOI: 10.32523/2306-6172-2024-12-2-81-91

1 Introduction

Multiscale methods are relevant in various fields where phenomena occur at multiple scales or levels of detail. In numerical simulations and modeling, multiscale methods are used to address problems that involve multiple spatial or temporal scales. By considering different scales simultaneously, these methods can provide a more comprehensive understanding of the system's behavior and capture important features that may be missed by traditional numerical methods. Overall, multiscale methods play an important role in bridging the gap between different scales of analysis, allowing for a more comprehensive understanding of complex systems [1, 2].

The contrast of parameters refers to significant variations or disparities in the properties or characteristics of the system being studied across different scales. This can include variations in material properties, boundary conditions, or other relevant parameters. The contrast of parameters strongly influences the solution of a multiscale problem. Multiscale methods are specifically designed to solve these problems by constructing basis functions that can efficiently handle parameter variations across different scales [3, 4].

Nevertheless, the high contrast of parameters can affect the choice of time integration schemes in time-dependent problems. Explicit time schemes rely on small time steps to ensure stability and accuracy. However, in the presence of high parameter contrast, the time step size may need to be further reduced to capture the fast dynamics associated with the high-contrast regions. This can significantly increase the computational cost and make the explicit time scheme impractical or inefficient for such problems.

In such cases, alternative time integration schemes, such as implicit or partially explicit methods, may be more suitable to handle the high contrast and ensure stability and efficiency [5]. For example, [6] proposes a new approach to solve the problem of poroelasticity in fractured media based on hybrid explicit-implicit learning (HEI). To facilitate the calculations, the authors use the fixed strain and fixed stress splitting schemes. The main idea of the proposed method lies in partial learning. The proposed splitting algorithm in [7] treats dominant multiscale modes in the implicit fashion, while the rest in the explicit fashion. The contrast-independent stability of these algorithms requires a special multiscale space design, which is the main purpose of the paper. It is shown that with an appropriate choice of multiscale spaces, an unconditional contrast stability can be achieved.

In this paper, we propose a multiscale approach with partially explicit time discretization. This approach is based on a meshfree generalized multiscale finite element method [8, 9]. The idea of the partially explicit scheme is to split the vector of coarse mesh solutions for the stiffness matrix into two parts: with fast processes (with fractures) and slow processes (without fractures). Next, use an implicit time scheme for nodes with fast processes, and an explicit time scheme for all others. In this way, it is possible to use a time step that is independent of the diffusion coefficient for fractures.

2   Problem formulation

In this paper, we consider the problem of single-phase filtration in a fractured porous medium. The mathematical model is described by a coupled system of differential equations for the pressure p_m in the porous matrix Ω and the pressure p_f in the fractures γ

$$
\begin{aligned}
c_m \frac{\partial p_m}{\partial t} - \operatorname{div}\left(\frac{k_m}{\mu} \operatorname{grad} p_m\right) + q(p_m - p_f) = 0, \quad x \in \Omega, \\
c_f \frac{\partial p_f}{\partial t} - \operatorname{div}\left(\frac{k_f}{\mu} \operatorname{grad} p_f\right) + q(p_f - p_m) = 0, \quad x \in \gamma,
\end{aligned}
\tag{1}
$$

where c_i is the media compressibility, k_i is the media permeability, μ is the fluid viscosity and q is the mass transfer coefficient ($i = m, f$).

System of equation (1) is supplemented by the initial and boundary conditions

$$
\begin{aligned}
p_i &= p_0, \quad t = 0, \\
p_m &= g, \quad x \in \xi, \\
p_f &= g, \quad x \in \xi, \\
-\frac{k_m}{\mu}(\operatorname{grad} p_m, n) &= 0, \quad x \in \partial\Omega, \\
-\frac{k_f}{\mu}(\operatorname{grad} p_f, n) &= 0, \quad x \in \partial\gamma.
\end{aligned}
$$

For our numerical tests, we take two different computational domains as shown in the Figure 2 to show the robustness of our proposed approach. Here, in the first geometry there are few fractures (Test 1), and in the second there is a more complicated permeability field with a large number of fractures (Test 2).

3   Fine-grid discretization

Let us define an uniform, for simplicity, time grid $\omega_t = \{t^n = n\tau,\ n = 0, 1, \ldots, N_t - 1,\ \tau N_t = t_{max}\}$, where τ - time step, N_t - number of time steps and t_{max} - solution time. Here we use the implicit time discretization of the system (1). For spatial approximation on a fine grid, we use the continuous Galerkin finite element method with standard linear basis functions (FEM). For the fractures accounting we use the discrete fracture model (DFM) [10, 11]. We use the superposition principle and assume that $p_1 = p_2 = p$. Then, summing the equations of the system (1), we obtain the following variational problem: find $p^{n+1} \in V$ such that

$$m(\frac{p^{n+1} - p^n}{\tau}, v) + a(p^{n+1}, v) = 0, \quad n = 0, 1, \ldots, N_t - 1,$$

where

$$m = m_1 + m_2, \quad a = a_1 + a_2,$$

$$m_1(\frac{p^{n+1} - p^n}{\tau}, v) = \int_\Omega c_m \frac{p^{n+1} - p^n}{\tau} v dx,$$

$$m_2(\frac{p^{n+1} - p^n}{\tau}, v) = \alpha \int_\gamma c_f \frac{p^{n+1} - p^n}{\tau} v ds,$$

$$a_1(p^{n+1}, v) = \int_\Omega \left(\frac{k_m}{\mu} \operatorname{grad} p^{n+1}, \operatorname{grad} v\right) dx,$$

$$a_1(p^{n+1}, v) = \alpha \int_\gamma \left(\frac{k_f}{\mu} \operatorname{grad} p^{n+1}, \operatorname{grad} v\right) ds,$$

(2)

where $\forall v \in \hat{V}$. Here $p^n \approx p(t^n)$ and α is the fracture aperture.

We build an unstructured mesh $\mathcal{T}_h$ and construct discrete function space $V_h \subset V$. Then we use $p_h = (p_{h,1}, p_{h,2}, \ldots, p_{h,Nf})^T$ to denote the vector of the required unknowns, where N_f – the number of fine mesh vertices. Next we write the following matrix form for the fully discrete system

$$M\frac{p_h^{n+1} - p_h^n}{\tau} + Ap_h^{n+1} = 0,$$

(3)

where

$$M = \{m_{ij}\}, \quad m_{ij} = m_1(\phi_j, \phi_i) + m_2(\hat{\phi}_j, \hat{\phi}_i),$$
$$A = \{a_{ij}\}, \quad a_{ij} = a_1(\phi_j, \phi_i) + a_2(\hat{\phi}_j, \hat{\phi}_i),$$

(4)

where ϕ_i – two-dimensional and $\hat{\phi}_i$ – one-dimensional fine-scale piecewise linear basis functions for the porous medium and fractures.

4 Meshfree GMsFEM

In this section, we give a brief description of the Meshfree GMsFEM algorithm for our problem. In offline stage we have the following steps

1. Generation of meshfree coarse grid depending on fractures.

2. Construction of a multiscale offline space.

3. Assembling a projection matrix into a multiscale offline space.

In the online stage, the fine-grid system is converted to a coarse grid system using the resulting projection matrix. As a result, the problem (2) is solved on a coarse grid.

4.1 Meshfree coarse scale

In Meshfree GMsFEM we use a point cloud instead of a structured triangular coarse grid. Let $\mathcal{S}_H$ be a partition of the computational domain Ω to the point cloud so that $\Omega \subset \bigcup_{i=1}^N S_i$ and suppose that each coarse element S_i is partitioned into a connected union of elements of a fine grid. Let $\{x_i\}_{i=1}^N$ is the coarse-scale nodes, where N denotes the number of coarse nodes. Here, the coarse elements S_i are the supports of basis functions

$$S_i = \{y \in \mathcal{R}^N : \parallel y - x_i \parallel \leq r_i\},$$

where r_i is radius of coarse element S_i.

We denote the basis functions by $\psi_{i,k}$, which is supported in S_i, and the index k represents the numbering of these basis functions. In turn, the solution will be sought as

$$p_c(x) = \sum_{i,k} c_{i,k} \psi_{i,k}(x). \tag{5}$$

Here the function $p_c(x)$ is general, referring to the pressure. This is due to the fact that the problem for the pressure is solved sequentially and for problem (2) the multiscale method will be almost the same. Where the multiscale method differs, we will point it out.

The main difficulties of the meshfree method are the choice of the location of points $\{x_i\}_{i=1}^N$, as well as the sizes of r_i for $\{S_i\}_{i=1}^N$. The version of CVT (centroidal Voronoi tessellations) proposed in [12] is used in this work. An important point here is the choice of the distribution density function $\rho(x)$. Here we calculate the distribution density function $\rho(x)$ of a random variable taking into account the fractures using the following problem

$$-\operatorname{div}(\beta \operatorname{grad}\rho) + \rho = f, \quad x \in \Omega,$$
$$-\beta \frac{\partial \rho}{\partial n} = 0, \quad x \in \partial\Omega, \tag{6}$$

where f is a piecewise linear function depending on the location of the fractures and β is a smoothing parameter, which in our case $\beta = 5$ was chosen by numerical experiments.

Here the right hand side in discrete form is defined as

$$f_h(x_i) = \begin{cases} 10^5, & x_i \in \gamma, \\ 1, & \text{otherwise}, \end{cases}$$

where $i = 1, 2, \ldots, N_f$ and N_f is a number of nodes of the fine grid. Next, we use the algorithm proposed in [13] for finding the radii r_i for S_i.

4.2 Local basis functions

To construct the offline space V_{off}^S, we solve the following local eigenvalue problem in each S_i

$$A\Psi^{\text{off}} = \lambda^{\text{off}} B\Psi^{\text{off}},$$

where A and B denote similar fine-scale matrices as

$$A = \{a_{ij}\}, \quad a_{ij} = \int_S (\lambda_1 \operatorname{grad} \phi_j, \operatorname{grad} \phi_i)\, dx + \alpha \int_{\gamma^S} \left(\lambda_2 \operatorname{grad} \hat{\phi}_j, \operatorname{grad} \hat{\phi}_i\right) ds,$$

$$B = \{b_{ij}\}, \quad b_{ij} = \int_S (\lambda_1 \phi_j, \phi_i)\, dx + \alpha \int_{\gamma^S} \left(\lambda_2 \hat{\phi}_j, \hat{\phi}_i\right) ds.$$

For definition of the multiscale basis functions, we select the first M eigenvectors corresponding to the first M smallest eigenvalues.

4.3 Global formulation

In the meshfree multiscale method the shape functions $W_i(x)$ defined in S_i form the initial coarse space

$$V_0^{\text{init}} = \operatorname{span}\{W_i(x)\}_{i=1}^N.$$

Here the shape functions $W_i(x)$ are defined as

$$W_i(x) = \frac{\phi_i(x)}{\sum_{j=1}^N \phi_j(x)},$$

where $\phi_i(x)$ are kernel functions, which here are cubic splines

$$\phi(r) = 2 \begin{cases} 2/3 + 4\,(r-1)\,r^2, & r \leq 0.5, \\ 4/3\,(1-r)^3, & 0.5 \leq r \leq 1, \\ 0, & 1 \leq r, \end{cases}$$

where r is the normalized distance.

Accordingly, by multiplying the form function $W_i(x)$ by the eigenvectors ψ_k^{off}, we obtain the basis functions in the offline space V_{off}

$$\psi_{i,k} = W_i \psi_k^{\text{off}}, \ 1 \leq i \leq N, \ 1 \leq k \leq M,$$

where k is an index of the eigenvector. Next, we construct the spectral multiscale space

$$V_{\text{off}} = \operatorname{span}\{\psi_{i,k} : 1 \leq i \leq N, \ 1 \leq k \leq M\}.$$

Also, for further use, an operator matrix is constructed

$$R^T = [\psi_1, \ldots, \psi_{N_c}],$$

where $N_c = N * M$ and ψ_i are used to denote the nodal values of each basis function defined on the fine grid. An example illustration of multiscale functions is shown in Figure 1.

The transition matrix R is then used to solve the following system on the coarse scale

$$M_c \frac{p_c^{n+1} - p_c^n}{\tau} + A_c p_c^{n+1} = 0, \tag{7}$$

where

$$M_c = RMR^T, \quad A_c = RAR^T.$$

After solving the system (7), we can go from a coarse-scale solution to a fine-scale solution using also the transition operator R and the solution p_c

$$p_{ms} = R^T p_c,$$

where p_{ms} is a fine-grid projection of the coarse-grid solution.
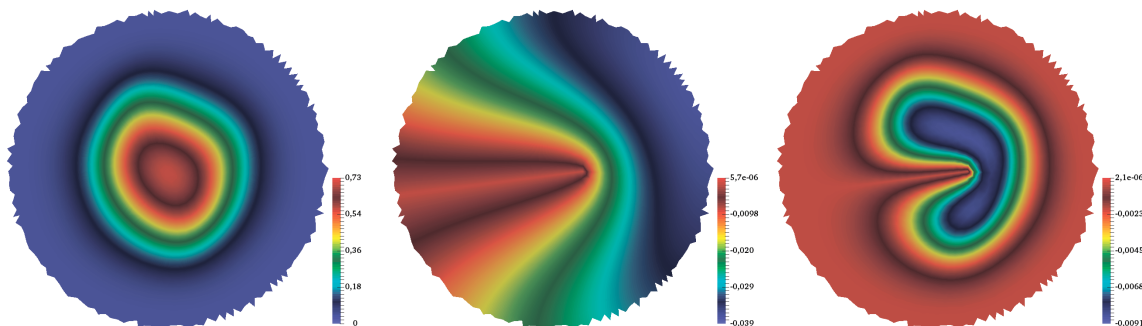

Figure 1: Illustration of multiscale functions. Left: shape function $W_i(x)$. Middle: eigenvector ψ_k^{off}. Right: multiscale basis function $\psi_{i,k}$.

4.4 Partially explicit scheme

Here we will discuss the time partially explicit scheme at the coarse mesh nodes. All indices and functions correspond to the coarse mesh only. First we have the discrete multiscale function space V_{off} and discrete solutions $p_c \in V_{off}$. We can represent the required function in the form of node values

$$p_c = \sum_{i=1}^{N} c_i \psi_i,$$

where for convenience, in contrast to the sum (5), we have reduced the index over the basis functions k, that is, $c_i = \sum_{j=1}^{M} c_i^j$ and $\psi_i = \sum_{j=1}^{M} \psi_i^j$. We use $p_c = (c_1, c_2, \ldots, c_N)^T$ to denote the vector of the required unknowns.

Let $N = N_I + N_E$, where N_I is the number of subdomains S_i that contain fractures, and N_E is the number without fractures. Then we can write

$$\sum_{i=1}^{N} c_i \psi_i = \sum_{i=1}^{N_I} c_i \psi_i + \sum_{i=N_I+1}^{N} c_i \psi_i,$$

or $p_c = (p_I, p_E)^T$, where $p_I = (c_1, c_2, \ldots, c_{N_I})^T$ and $p_E = (c_{N_I+1}, c_{N_I+2}, \ldots, c_N)^T$. Then, we have following system for the multiscale problem: find $p_c^{n+1} \in V_H$ such that

$$M_c \frac{p_c^{n+1} - p_c^n}{\tau} + A_c \begin{pmatrix} p_I^{n+1} \\ p_E^n \end{pmatrix} = 0, \quad n = 0, \ldots, N_t - 1,$$

where p_I^{n+1} corresponds to implicit part of calculations, and p_E^n to explicit ones. Thus we obtain a partially explicit scheme in time. The Figure 2 shows which nodes correspond to the solutions p_I and p_E for Test 1 and Test 2.
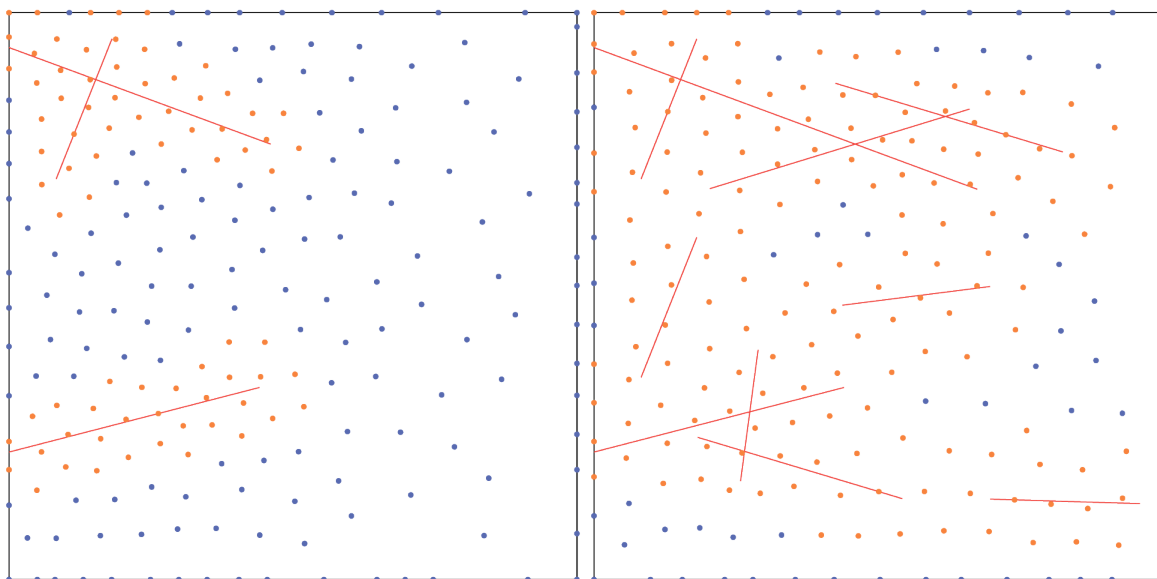

Figure 2: Illustration of computational domains Ω with the fractures γ (red lines) and point clouds with $N = 225$, where orange dots are nodes for p_I and blue dots are nodes for p_E. Left: Test 1 with $N_I = 77$ and $N_E = 148$. Right: Test 2 with $N_I = 160$ and $N_E = 65$.

5   Numerical results

This section presents numerical results for a single-phase filtration problem in a fractured porous medium, demonstrating that the proposed approach can predict an accurate approximation of the solution, independent of the contrast. The two-dimensional model problem defined in $\Omega = [0, 80] \times [0, 80]$ was considered. The fine meshes for Test 1 and Test 2 are similar and have 34,814 vertices and 68,983 elements and 34,949 vertices and 69,253 elements, respectively. For both tests in the multiscale method we

use $N = 225$ and $M = 6$. For Test 1 we use $N_I = 77$ and $N_E = 148$ and for Test 2 we use $N_I = 160$ and $N_E = 65$.

The problem was solved numerically with the following values of the parameters: $c_m = 0.4$, $c_f = 1$, $k_m = 10^{-2}$, $k_f = 10^3$, $\alpha = 1$, $\mu = 1$, $p_0 = 1$, $g = 10$, $t_{max} = 900$, $N_t = 300$, $\tau = 3$.

To approximate equations using the finite element method on a fine grid, construct systems and solve them, we use the open source computing platform FEniCS [14] (LGPLv3).

Figure 3 show the solutions at the final time for Test 1 and Test 2. As we can see, the solutions obtained by multiscale methods with implicit and partially explicit discretization are similar to the reference solution on a fine grid.
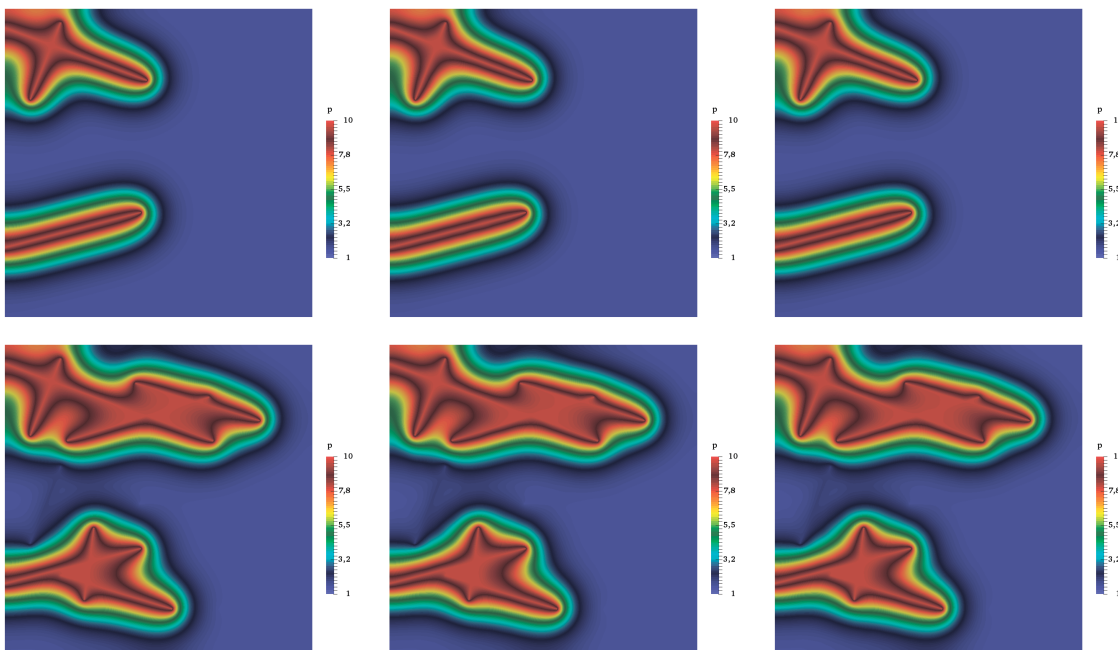

Figure 3: Solutions at the final time for Test 1 (Top) and Test 2 (Bottom). Left: reference solutions. Middle: Meshfree GMsFEM with impicit method. Right: Meshfree GMsFEM with partially explicit method.

To test our approach, we compare the solution obtained on a coarse grid with the solution obtained on a fine grid. The relative errors in L^2 and H^1 are calculated at each time as follows in percentages

$$||e||_{L^2} = \sqrt{\frac{||u_1 - u_2||_{L^2}}{||u_1||_{L^2}}} \times 100\%, \quad ||e||_{H^1} = \sqrt{\frac{||u_1 - u_2||_{H^1}}{||u_1||_{H^1}}} \times 100\%,$$

where $||u||_{L^2} = \int_\Omega u^2 dx$, $||u||_{H^1} = \int_\Omega (\operatorname{grad} u, \operatorname{grad} u) dx$, u_1 – fine-grid solution and u_2 – multiscale solution.

Figures 4 show the relative errors in L^2 and H^1 of the meshfree multiscale method with an implicit time scheme for Test 1 and Test 2. As we can see, the errors fall over

time and in the end become less than 0.5% in L^2 and 4% in H^1 for both tests. This indicates that the proposed meshfree multiscale approach can achieve good accuracy with a small number of degrees of freedom.
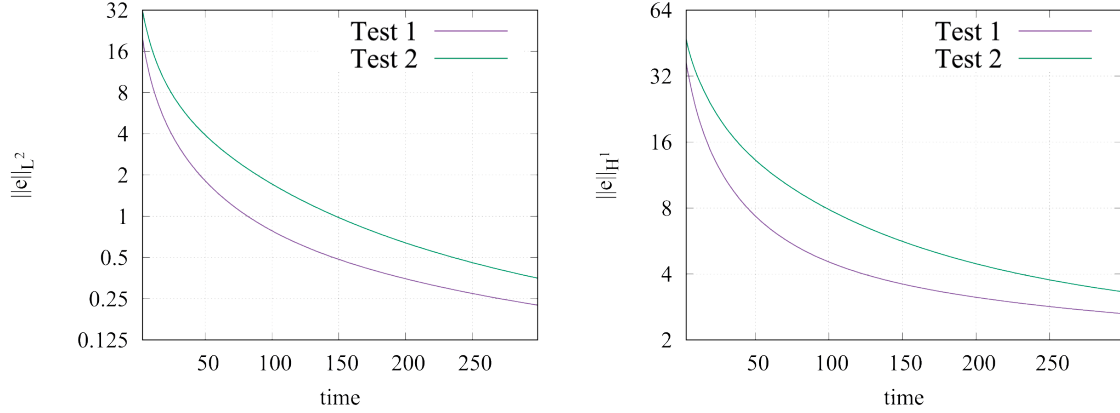

Figure 4: Plots of relative errors in L^2 (left) and H^1 (right) compared to the reference solution.

In Figures 5 we plot the relative errors of the solution obtained with the partially explicit scheme versus the solution with the implicit time scheme. Here we see that the errors in L^2 do not exceed 0.6% for both tests, and in H^1 they do not exceed 3.5% for Test 1 and 2% for Test 2. Here, the number of nodes N_I and N_E for a partially explicit scheme have an influence, but it is insignificant, since for Test 1 we took twice as many nodes for the explicit part as for the implicit part and obtained good results.
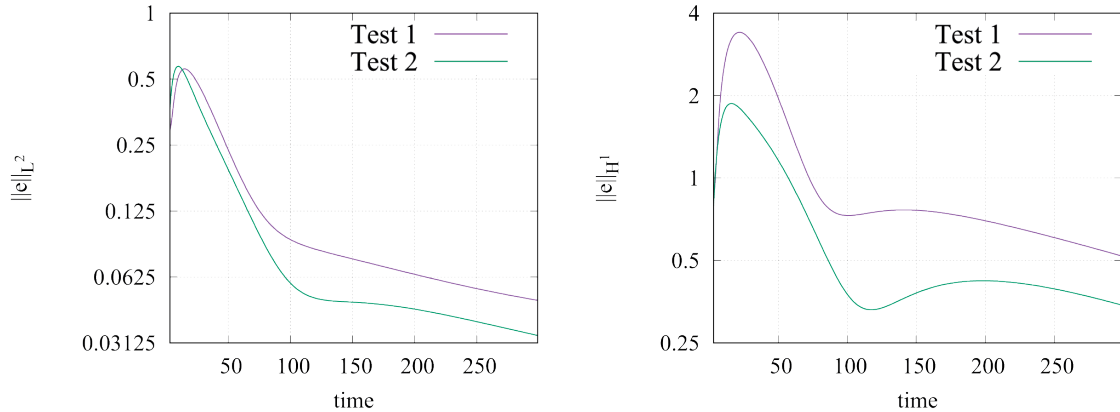

Figure 5: Plots of relative errors in L^2 (left) and H^1 (right) between impicit and partially explicit methods.

6   Conclusion

In this paper, a time partially explicit scheme is proposed for the meshfree generalized multiscale finite element method. This scheme does not depend on the high contrast of the multiscale problem, but depends only on the permeability of the porous medium, which is much less than the permeability of fractures. It is shown numerically that our chosen partially explicit scheme provides reliable time discretization. The developed time discretization is beneficial for meshfree multiscale methods or other approaches that control the location of coarse mesh nodes to achieve high computational accuracy.

Acknowledgement

References

[1] Efendiev Y., Hou T. Y., *Multiscale finite element methods: theory and applications*, Springer Science & Business Media, 4 (2009).

[2] Chung E., Efendiev Y., Hou T. Y., *Multiscale Model Reduction: Multiscale Finite Element Methods and Their Generalizations*, Springer Nature, 212 (2023).

[3] Stepanov S., Nikiforov D., Grigorev A., *Multiscale Multiphysics Modeling of the Infiltration Process in the Permafrost*, Mathematics, 9.20 (2021), 2545.

[4] Ammosov D., Vasilyeva M., Chung E. T., *Generalized Multiscale Finite Element Method for thermoporoelasticity problems in heterogeneous and fractured media*, Journal of Computational and Applied Mathematics, 407 (2022), 113995.

[5] Vabishchevich P. N., *Additive Operator-Difference Schemes: Splitting Schemes*, Walter de Gruyter, (2013).

[6] Ammosov D. , Grigorev A., Stepanov S., Tyrylgin A., *Partial learning using partially explicit discretization for multicontinuum/multiscale problems. Fractured poroelastic media simulation*, Journal of Computational and Applied Mathematics, 424 (2023), 115003.

[7] Chung E. T., Efendiev Y., Leung W. T., Vabishchevich P. N., *Contrast-independent partially explicit time discretizations for multiscale flow problems*, Journal of Computational Physics, 445 (2021), 110578.

[8] Nikiforov D., *Meshfree Generalized Multiscale Finite Element Method*, Journal of Computational Physics, 474 (2023), 111798.

[9] Nikiforov D. Y., Stepanov S. P., *Modeling of Artificial Ground Freezing Using a Meshfree Multiscale Method*, Lobachevskii Journal of Mathematics, 44.3 (2023), 1206-1214.

[10] Vasil'eva M. V., Vasiliev V. I., Krasnikov A. A., Nikiforov D. Y., *Numerical simulation of single-phase fluid flow in fractured porous media*, Uchenye Zapiski Kazanskogo Universiteta. Seriya Fiziko-Matematicheskie Nauki, 159.1 (2017), 100-115.

[11] Vasil'ev V. I., Vasil'eva M. V., Gladkikh V. S., Ilin V. P., Nikiforov D. Y., Perevozkin D. V., Prokop'ev G. A., *Numerical solution of a fluid filtration problem in a fractured medium by using the domain decomposition method*, Journal of Applied and Industrial Mathematics, 12.4 (2018), 785-796.

[12] Ju L., Du Q., Gunzburger M., *Probabilistic methods for centroidal Voronoi tessellations and their parallel implementations*, Parallel Computing, 28.10 (2002), 1477-1500.

[13] Griebel M., Schweitzer M. A., *A particle-partition of unity method for the solution of elliptic, parabolic, and hyperbolic PDEs*, SIAM Journal on Scientific Computing, 22.3 (2000), 853-890.

[14] Logg A., Mardal K. A., Wells G. (ed.), *Automated solution of differential equations by the finite element method: The FEniCS book*, Springer Science & Business Media, 84 (2012).

D. Y. Nikiforov,
North-Eastern Federal University,
NEFU, Belinsky St., 58, Yakutsk 677000, Russia,
Email: `dju92@mail.ru`,